

# Microseismic characterization of brittle fracture mechanism in highly stressed surrounding rock mass

## Chunchi Ma

State Key Laboratory of Geohazard Prevention and Geoenvironment Protection, Chengdu University of Technology, No.1 ErXianQiao Road, Chengdu, China  
nanjiguang1017@sina.com

## Yupeng Jiang\*

Centre for Geoscience Computing, School of Earth Sciences, The University of Queensland, Room.257, Steel Building, St. Lucia, Brisbane, Australia  
yupeng.jiang@uq.net.au

## Tianbin Li

State Key Laboratory of Geohazard Prevention and Geoenvironment Protection, Chengdu University of Technology, No.1 ErXianQiao Road, Chengdu, China

## Guoqing Chen

State Key Laboratory of Geohazard Prevention and Geoenvironment Protection, Chengdu University of Technology, No.1 ErXianQiao Road, Chengdu, China

### SUMMARY

Brittle fracturing of rock mass is a major problem for deep tunnelling or mining in highly stressed rock mass, which could evolve into rockburst hazard and severely undermine the safety of engineering project. In this paper, an advanced microseismic approach is proposed to analyse the mechanism clearly. The results suggest that brittle fracturing contains three energy development stages (i.e. energy accumulation, energy transfer and energy release). Therefore, based on the seismic energy moment and the apparent stress criteria, microseismic events can be classified into six categories that corresponding to the three major categories of stress-adjustment event, deformation-driven event and bursting event. The Energy index develops steadily at first, then followed by a drastic drop and finally ends with a large increment. Cumulative apparent volume grows slowly before a sudden increase. For brittle fracturing development, tensile cracks appear firstly, then the shear cracks and finally the mixed types of cracks.

**Key words:** Brittle fracturing mechanism, Microseismic characterization, Energy stages, Rock mass behaviour

### INTRODUCTION

Brittle fracture is a unique rock behaviour that commonly occurred in highly-stressed hard brittle rock. Differing from ductile fracture, brittle fracture has the characteristics of unobvious deformation before rupturing, good energy storage capability, quickly dissipating stress and high energy release (Bieniawski 1967a, 1967b). Microseismic events induced by brittle fracture have unique features in source mechanisms and source parameters. Therefore, it is feasible to utilize the microseismic related method to analyse and predict the brittle fracturing behaviour in rock mass.

The existing literatures about this issue are mainly focused on the outcome of brittle fracturing, i.e. the assessment of rockburst hazard (Srinivasan 1997; Eneva et al. 1998). However, rockburst hazard can be regarded as the evolutionary result of brittle fracturing (Ma et al. 2015). It would be more accurate and informative to analyse the rock mass behaviour with direct microseismic characterization of brittle fracture mechanism. Hence, this paper proposed an advanced method for the characterization of the progress of brittle fracturing. This method was applied in a deep tunnelling project and the responded microseismic events of surrounding rock mass are studied. Microseismic events are classified to describe different stages of brittle fracturing; microseismic source parameters and source types during the process of brittle fracturing are analysed. The results suggest that predictions for brittle fracturing or rockburst hazard can be highly improved by these analyses.

### METHODS AND RESULTS

Microseismic monitoring technology was conducted in the tunnelling of the Zijing tunnel on the Yingxiu-Wolong highway in Southwest China. Measurements of the stress field for this tunnel (section: K13+670~K13+770) gave readings of: maximum principle stress 29.2 MPa, intermediate principle stress 16.4 MPa, and minimum principle stress 14.6 MPa. The direction of the maximum principle stress is nearly perpendicular to the axial direction of tunnel. The dip angles of the three principle stresses are 3°, 87°, and 0°. The stratum of the tunnel field is mainly diorite, hard, and brittle

Microseismic Event Classification

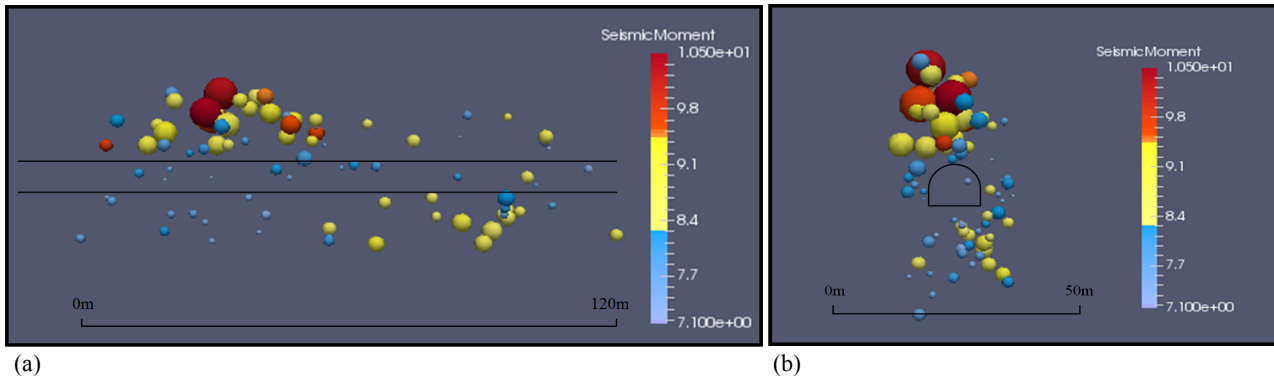


Figure 1: Monitored micro-seismic events in section K13+670~770, (a): longitudinal perspective of a tunnel, (b) transverse perspective of a tunnel

Figure 1 shows the excavation induced microseismic events during the process of tunnelling, seismic moment is distinguished by colours and seismic energy is distinguished by ball sizes. Every event can be characterized in the energy versus seismic moment space (Figure 2). Three assessment criteria: seismic energy  $E$ ; seismic moment  $M_o$ ; and apparent stress  $\sigma_a$  are used to define the classification of microseismic events. The apparent stress parameter, which is a measure of the average co-seismic stress adjustment, is proportional to stress drop  $\Delta\sigma$  and a more reliable parameter:

$$\sigma_a = G \frac{E}{M_o} \propto \Delta\sigma = \frac{7M_o}{16r_o^3} \tag{1}$$

where  $G$  denotes shear modulus of rock mass,  $r_o$  denotes source radius.

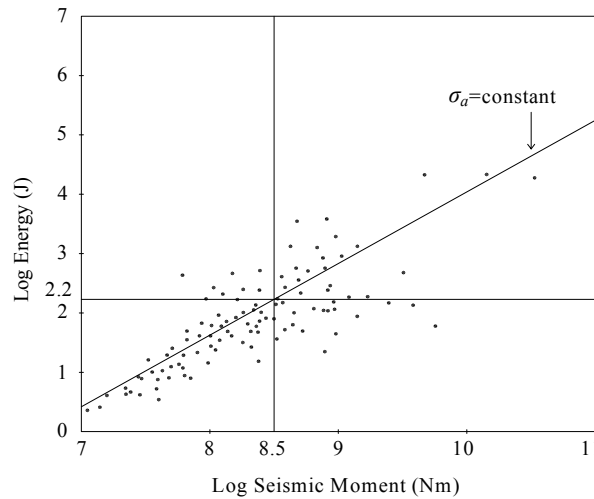


Figure 2: Seismic energy moment mapping of microseismic event

As shown in Figure 2 thresholds of log seismic energy and log seismic moment are picked as 2.2 and 8.5 respectively. Microseismic events are gathering around the constant value (7700pa) of apparent stress. The distribution of microseismic events in  $\log E$ - $\log M_o$  coordinate system can be divided into six categories (Figure 3):

- Type I, microseismic events are located below  $E$  threshold and  $M_o$  threshold, above  $\sigma_a$  threshold, indicating the small deformation events with relatively high energy level.
- Type II, microseismic events are located below  $E$  threshold,  $M_o$  threshold and  $\sigma_a$  threshold, indicating the small deformation events with low energy level.
- Type III, microseismic events are located below  $\sigma_a$  threshold, above  $E$  threshold and  $M_o$  threshold, indicating the large deformation events with relatively low energy level (even though the absolute value of energy is large).
- Type IV, microseismic events are located below  $E$  threshold and  $\sigma_a$  threshold, above  $M_o$  threshold, indicating the large deformation events with low energy level.
- Type V, microseismic events are located above  $E$  threshold,  $M_o$  threshold and  $\sigma_a$  threshold, indicating the large deformation events with high energy level.
- Type VI, microseismic events are located below  $M_o$  threshold, above  $\sigma_a$  threshold and  $E$  threshold, indicating the small deformation events with high energy level.

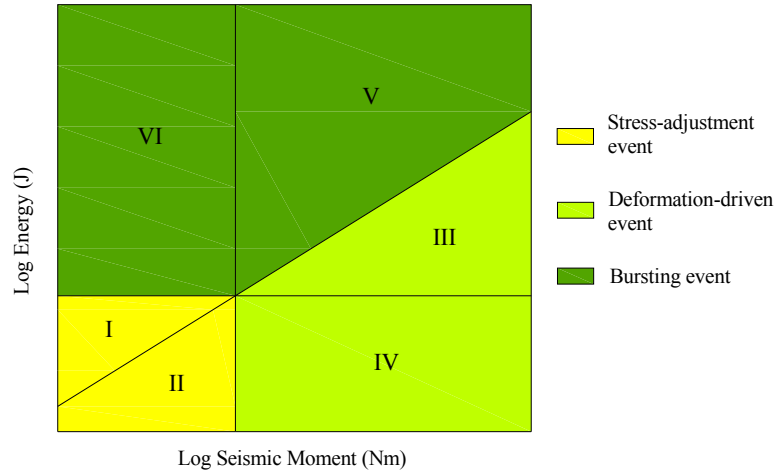


Figure 3: Classification of microseismic events

These six categories of microseismic events can be further classified into three major categories (Figure 3): Stress-adjustment event, Deformation-driven event and Bursting event. Stress-adjustment events (containing Type I and Type II) occur due to unloading of highly-stressed rock mass and energy accumulation. As the inelastic deformation constantly increasing and rock damage accumulating, larger co-seismic deformation events (deformation-driven event, containing Type III and Type IV) occur to strain the rock mass more, resulting in stress redistribution and energy transfer to surrounding rock mass. Eventually, macroscopic fracture forms and huge amounts of energy release to make bursting events (containing Type V and Type VI) happen. Thus the occurrence of microseismic events responds to the three stages of brittle fracturing, energy accumulation, energy transfer and energy release.

Microseismic Source Mechanism Analysis

Source parameters of energy index and apparent volume are used to depict the process of brittle fracturing. The notion of comparing the radiated energies of microseismic events of similar potency can conveniently be translated into a practical tool called the energy index,  $EI$ . The energy index of an event is the ratio of the observed radiated seismic energy of that event  $E$ , to the average energy  $E(P)$  radiated by events of the observed potency  $P$  for the area of interest.

$$EI = \frac{E}{E(P)} = \frac{E}{10^{d \log P + c}} = 10^{-c} \frac{E}{P^d} \tag{2}$$

where  $P$  denotes seismic potency,  $d$  and  $c$  are relevant coefficients.

Apparent volume measures the volume of rock with the inelastic strain change:

$$V_A = \frac{P}{\epsilon_A} = \frac{\mu P^2}{E} \tag{3}$$

where  $\epsilon_A$  denotes apparent strain,  $\mu$  denotes rigidity of rock.

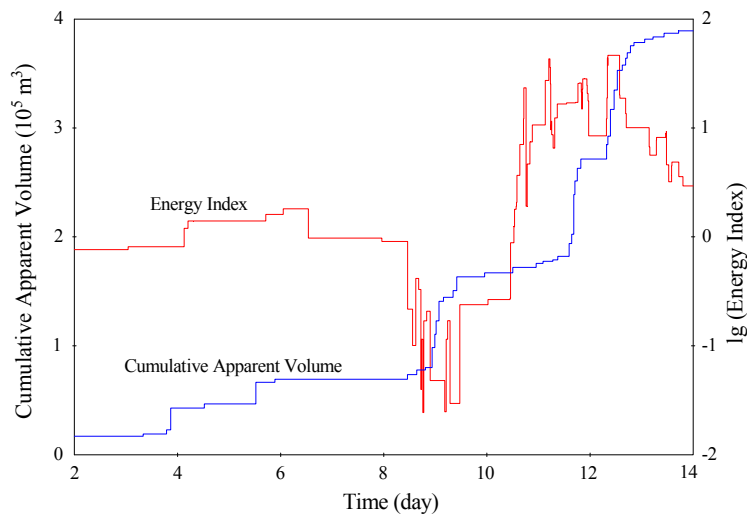


Figure 4: Time histories of energy index and cumulative apparent volume

Based on the source parameters proposed above, the time histories of energy index and cumulative apparent volume during the progress of brittle fracturing possess the following three stages (Figure 4 and 5): Stage one, steadily increasing energy index and cumulative apparent volume. Stage two, quickly dropping energy index and simultaneously accelerating cumulative apparent volume. Stage three, quickly increasing energy index and cumulative apparent volume.

Aside from source parameters, source types of microseismic event are also parameterized from the moment tensor analysis. The full moment tensor has three eigenvalues:  $m_1$ ,  $m_2$  and  $m_3$ , each of them determines the component of isotropic, compensated linear vector dipole, and double-couple respectively. The isotropic component is described by the trace of tensor ( $3m = m_1 + m_2 + m_3$ ) and the deviatoric components are defined as:

$$m'_1 = m_1 - m \quad m'_2 = m_2 - m \quad m'_3 = m_3 - m \quad (4)$$

These deviatoric components are ordered as  $|m'_1| < |m'_2| < |m'_3|$  according to Hudson et al (1989). The source types of microseismic event could be parameterized in terms of the quantities  $k$  and  $T$ , respectively:

$$k = \frac{m}{|m| + |m'_3|} \quad T = \frac{2m'_1}{|m'_3|} \quad (5)$$

Both quantities vary between -1 and 1. A source with  $k=1$  corresponds to a purely explosive event, while one with  $k=-1$  corresponds to a pure implosion. The  $T=1$  and -1 correspond to sources where one strain axis is shortening while the other two are lengthening, or vice versa. All pure double-couple sources are uniquely described by  $k=T=0$ .

The variety of source mechanisms can be discriminated in the source-type diagram. Figure 5 shows the three stages of source-type diagram corresponding to the time histories of energy index and cumulative apparent volume. Stage one, events are clustering near the point of tensile crack opening, sparse events are distributed at the right part. Stage two, events are clustering around the point of double couple, indicating the main source types are shear failure. Stage three, events are distributed between the points of tensile crack opening and double couple, indicating the source types are combined of shear, tensile and tensile-shear failures.

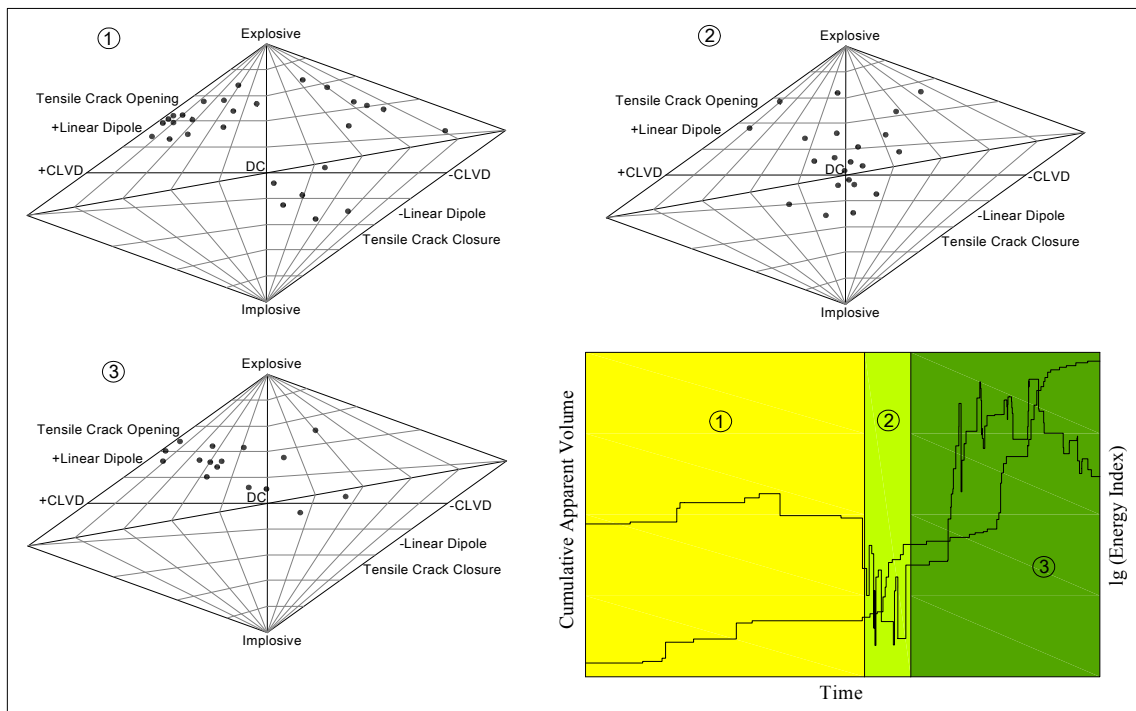


Figure 5: Source type diagrams during brittle fracture

### CONCLUSIONS

Brittle fracture is a dynamic rock behaviour containing the process of energy accumulation, energy transfer and energy release. The comprehensive microseismic method has been utilized to characterize this mechanism.

- 1) Based on the evaluation of seismic energy, seismic moment and apparent stress, brittle fracturing released microseismic events could be classified into stress-adjustment events, deformation-driven events, and bursting events.
- 2) According to the time histories of energy index and cumulative apparent volume, energy index increases steadily at first, then decreases quickly and finally re-increases largely; cumulative apparent volume grows slowly before a sudden increase. This process indicates the deterioration of rock mass from strain hardening, strain softening to rupturing, and the migration of energy.
- 3) As brittle fracturing develops, tensile cracks appear firstly, then the shear cracks and finally the mixed cracks of tensile, shear and tensile-shear.

### ACKNOWLEDGMENTS

The authors want to express their thanks to the staff from China Railway Bureau who provide their kind help for the microseismic monitoring as well as the collaborative funding support from National Natural Science Foundation of China (Grant Nos. 41230635 and 41172279).

### REFERENCES

- Bieniawski, Z.T., 1967, Mechanism of brittle fracture of rock, PartI-theory of the fracture process. *Int J Rock Mech Min Sci* 4:395–406
- Bieniawski, Z.T., 1967, Mechanism of brittle fracture of rock, PartII-experimental studies. *Int J Rock Mech Min Sci* 4:407–411
- Ma, C.C., Li, T.B., Cheng, G.Q., Cheng, Z.Q., 2015, Study of micro particle model for hard brittle rock and the effect of unloading rock burst. *Chinese Journal of Rock Mechanics and Engineering* 34:1–11
- Srinivasan, C., Arora, S.K., Yaji, R.K., 1997, Use of mining and seismological parameters as premonitors of rockburst. *Int J Rock Mech Min Sci* 34:1001–8
- Eneva, M., Mendecki, A., Van, A.G., 1998, Seismic response of rock mass to blasting and rockburst potential. *Int J Rock Mech Min Sci* 35:390–1
- Hudson, J., Pearce, R., Rogers, R., 1989, Source type plot for inversion of the moment tensor, *Journal of Geophysical Research* 94:765-774